

Validating a Nonhuman Primate Model of Super-Selective Intraophthalmic Artery Chemotherapy: Comparing Ophthalmic Artery Diameters

Lauren C. Ditta,¹ Asim F. Choudhri,²⁻⁴ Brian C. Tse,¹ Mark M. Landers,⁵ Barrett G. Haik,^{1,6} Jena J. Steinle,¹ J. Scott Williams,² and Matthew W. Wilson^{1,6,7}

PURPOSE. Superselective intraophthalmic artery chemotherapy (SSIOAC) is being used for treatment of retinoblastoma; however, the hemodynamic consequences and toxicities are not fully known. We developed a nonhuman primate (NHP) model of SSIOAC and reported our clinical observations. For validation, we compared ophthalmic artery (OA) diameters between NHPs and children (<6 years).

METHODS. Endovascular cannulation of the right OA was performed three times each in six adult male Rhesus macaques. Angiographic OA images were obtained and measured, and postmortem OAs were histologically sectioned and measured. Retrospectively, computed tomography (CT) and magnetic resonance (MR) angiography images of the head in children and adolescents (as an adult reference) were used to measure the OA luminal diameter at its origin.

RESULTS. The median angiographic diameter of treated NHP OA origins ($n = 6$) was 1.06 mm (range 0.94–1.56). Histologic measurements (8 of 12 NHP OAs) gave a median diameter of 1.09 mm (range 0.95–1.41). In 98 children (from 169 consecutive CT and MR angiography studies; median age 1.01 years, range 0.01–5.74), 186 OAs were measurable at the origin (median luminal diameter 1.28 mm, range 0.82–2.00; $P = 0.16$ for the angiographic NHP diameters versus pediatric cohort). Angiographic measurements of 34 OAs (of 20 consecutive studies of adolescents; median age 16.55 years, range 14.40–18.18) gave a median luminal diameter of 1.45 mm (origin, range 1.13–1.66; $P < 0.0001$, adolescent versus pediatric).

CONCLUSIONS. Measurements of the OA luminal diameter at its origin were similar between our NHP and pediatric cohort,

validating our NHP model for testing both the hemodynamic consequences and toxicities of SSIOAC. (*Invest Ophthalmol Vis Sci.* 2012;53:7791–7794) DOI:10.1167/iovs.12-10605

Primarily, the treatment of retinoblastoma aims to save lives; secondarily, to save the eye and preserve vision. Retinoblastoma treatment has evolved over the past several decades: from external beam radiation to intravenous systemic chemotherapy to localized chemotherapy through arterial cannulation of the internal carotid system. Therapies have shifted to place more emphasis on globe salvage. Superselective intraophthalmic artery chemotherapy (SSIOAC) is currently being used for the treatment of retinoblastoma. SSIOAC, a technique modeled from the early work of Kaneko,¹ delivers a high dose of intraocular concentrations of chemotherapeutic agents by direct cannulation of the ophthalmic artery (OA), thus reducing unwanted systemic toxicities. Since 2008, SSIOAC has been used at select institutions for treatment of advanced retinoblastoma,² and it has been increasingly offered for the treatment of certain primary or secondary tumors.^{3–11} While SSIOAC has proven to demonstrate remarkable tumor regression, an increasing number of institutions are reporting cases of retinal toxicity, vascular damage, and ocular morbidity.^{5–8,12–18}

SSIOAC may offer a theoretical advantage in the treatment of retinoblastoma, yet further investigation is needed to master the technical aspects of the procedure, to understand the hemodynamic consequences of endovascular cannulation, and to define drug toxicities.

To study and better understand SSIOAC, we developed a nonhuman primate (NHP) model to observe, with real-time imaging, the consequences of SSIOAC.^{19,20} To validate our model, we compared OA diameters between our NHPs and a cohort of children less than 6 years of age.

METHODS

Nonhuman Primate Model

Approval was received from the institution's animal care and use committee. All animals were treated in accordance with ARVO Statement for the Use of Animals in Ophthalmic and Vision Research. Endovascular cannulation of the right OA was performed three times each in six adult male Rhesus macaques (*Macaca mulatta*, median age 10.5 years, median weight 11.6 kg, median eye measurements $19 \times 19 \times 19$ mm) for 18 total procedures. Lateral projection angiographic images were obtained prior to each of the three infusions for all animals. Measurements of the NHP OA diameter were made from these images at the first location after the origin, whereby the vessel could be clearly seen in profile without obscuration by mixing of

From the ¹Department of Ophthalmology, Hamilton Eye Institute, and the Departments of ²Radiology, ³Neurosurgery, and ⁵Comparative Medicine, University of Tennessee Health Science Center, Memphis, Tennessee; the ⁴Le Bonheur Neuroscience Institute, Le Bonheur Children's Hospital, Memphis, Tennessee; and the ⁶Department of Surgery, Division of Ophthalmology, and the ⁷Department of Pathology, St. Jude Children's Research Hospital, Memphis, Tennessee.

Presented at the Association for Research and Vision in Ophthalmology, Ft. Lauderdale, Florida, May 7, 2012.

Supported by Research to Prevent Blindness, Inc., New York, New York and the St. Giles Foundation, New York, New York.

Submitted for publication July 17, 2012; revised September 22, 2012; accepted October 24, 2012.

Disclosure: L.C. Ditta, None; A.F. Choudhri, None; B.C. Tse, None; M.M. Landers, None; B.G. Haik, None; J.J. Steinle, None; J.S. Williams, None; M.W. Wilson, None

Corresponding author: Matthew W. Wilson, Hamilton Eye Institute, 930 Madison, Room 476, Memphis, TN 38163; mwilson5@uthsc.edu.

contrast and unopacified blood, typically within 2 to 4 mm of the origin (Fig. A).

Postmortem dissection of the monkeys was performed after the third SSIOAC treatment. Using a 15-blade scalpel, the scalp of the monkey was reflected to expose the skull. The calvarium was then removed using a bone saw. The brain was removed, taking care to preserve the Circle of Willis and optic nerves. Dura was stripped from the skull base using rongeurs. Rongeurs were then used to remove the roofs of the orbit and optic canal. The levator and superior rectus muscles were reflected using Westcott scissors. Orbital fat was dissected off the vasculature using Jeweler's forceps. The OA and its branches were identified. The optic nerves were carefully removed and preserved in formalin to reveal the origin of the OA. The orbital arterial tree was removed en bloc from the right and the left orbits of each monkey and placed into 10% neutral buffered formalin. Sections over the entire length of the ophthalmic, central retinal, and lacrimal arteries were placed in paraffin blocks and then serially sectioned for staining with hematoxylin and eosin. Every fifth section was stained and examined. Ten measurements of the luminal diameter were taken along the entire length of each OA to yield an average diameter (Olympus DP Controller [DP-BSW], ver. 3.3.1.292, Olympus Corporation, Center Valley, PA). Average diameters were obtained for eight of the 12 eyes dissected, with tissue sections from the other four eyes unavailable due to processing difficulties.

Noninvasive Analysis of Human Pediatric Ophthalmic Artery

For comparison, we performed an Institutional Review Board-approved retrospective analysis of computed tomography (CT) and magnetic resonance (MR) angiography of the head in children less than 6 years of age. A Healthcare Information Portability and Accountability Act-compliant database was searched to identify appropriate studies for review between 2006 and 2011. Using the same database, we also identified 20 consecutive adolescents with measurable vasculature to use as adult references. The studies were consecutive studies. Excluded CT and MR studies included MR venograms, nonvisualization of the OA, excessive motion artifact, high-flow intracranial vascular malformation, carotid artery pathology such as dissection or moyamoya, and duplicate studies on a single patient. Additionally, patients with retinoblastoma or other orbital tumors, infections, and vascular abnormalities were excluded from the study.

Measurements of the OA luminal diameter on CT and MR studies were made in a plane perpendicular to the long-axis of the artery shortly after the origin at the first location where there was no longer rapid tapering of the vessel, usually within 2 mm of the origin (Fig. B). This was confirmed on sagittal, coronal, and oblique multiplanar reconstructions of the volumetric datasets including use of maximal-intensity projections to allow measurement of the true diameter without overestimation of size due to vessel tortuosity and without underestimation of size due to volume-averaging (Figs. C, D).

Statistics

Data was collected in a spreadsheet application (Microsoft Excel; Microsoft, Inc., Redmond, WA). Statistical calculations were made using a spreadsheet application (Microsoft Excel [Microsoft, Inc.] and SPSS [IBM Corp., Armonk, NY]). A two-tailed Student's *t*-test was used to compare the size of the origin of the OA in the NHPs and the pediatric patients. Serial measurements were analyzed using repeated-measures ANOVA. Also, comparisons were made between the pediatric and adolescent populations at the measurable anatomical locations of the OA in its course to supply the orbit.

RESULTS

In the NHPs, the median angiographic diameter of the OA origin of the six treated right OAs was 1.06 mm (range 0.94 to

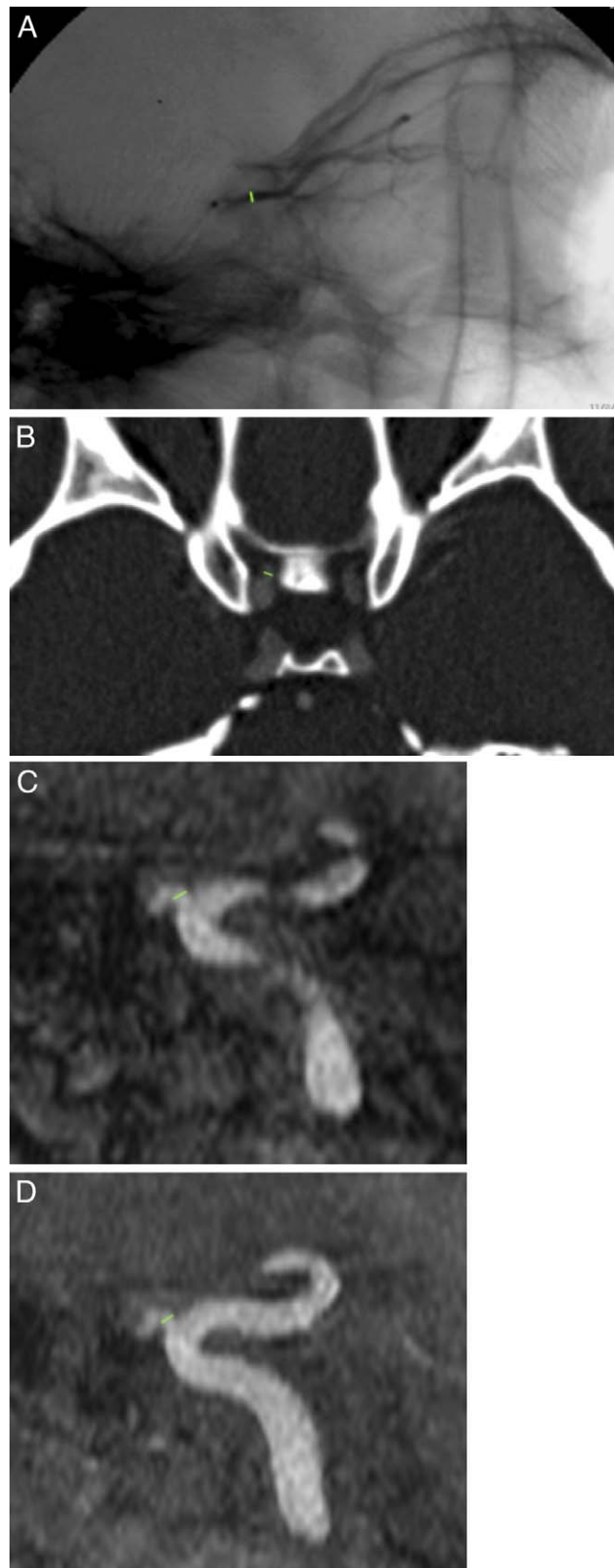


FIGURE. Lateral image of a super-selective angiogram of a NHP OA (A), with a measurement between the level of the ophthalmic origin and the orbital apex. Axial CT angiographic image showing a measurement of the OA diameter shortly after the origin (B). A sagittal reformat of an MR angiogram (C) as well as a sagittal maximum-intensity projection of the same MR angiogram (D) demonstrating the location of the measurement.

–1.56; mean 1.18 ± 0.26 mm). There were no significant changes between the first, second, or third measurement in any of the macaques ($P = \text{NS}$). We successfully measured 8 of 12 OAs on histology sections obtaining a median diameter of 1.09 mm (range 0.95–1.41, mean 1.15 ± 0.24 mm). There was no significant difference between the angiographically and histologically measured OA diameters ($P = 0.78$). We identified 169 consecutive CT and MR angiography studies of the head in children less than 6 years of age. In 98 of these pediatric patients (48 females, median age 1.01 years [range 0.01–5.74; mean 1.36 ± 1.40 years]), 186 OAs were measurable at its origin off the internal carotid artery with a median luminal diameter of 1.28 mm (range 0.82–2.00; mean 1.29 ± 0.16 mm). There was no significant difference in angiographic OA diameter between our NHP and pediatric cohorts ($P = 0.16$).

In the adolescent group, median age of the 20 adolescents (11 females) was 16.55 years (range 14.40–18.18; mean 16.36 ± 0.99 years), 34 OA origins in 18 patients were measurable, with a median luminal diameter of 1.45 mm (range 1.13–1.66; mean 1.42 ± 0.11 ; $P < 0.0001$, adolescent versus pediatric). There was no significant difference between right and left in any of the measurements made within each age group ($P = \text{NS}$).

DISCUSSION

In our current study, we sought to validate our NHP model by evaluating the size of the pediatric and adolescent OAs and comparing it to the OA size in the macaques.

SSIOAC for the treatment of retinoblastoma has the potential to improve outcomes with decreased morbidity; however, many questions remain unanswered. Without the benefit of a prospective clinically controlled trial, it is unclear if SSIOAC is a translatable technique.²¹ We developed the NHP model to study the real-time consequences of SSIOAC. We chose this primate for several reasons. Previous studies demonstrate the macaque as an acceptable animal model for medical research because of its anatomic and physiologic similarity to the human. Specifically, the Rhesus macaque's cephalic arterial system is almost identical to that of a human being, with no major differences in the origin or branching pattern of the OA.²³

The adult male Rhesus macaque is comparable in weight and size to a 2-year-old human being, the age of a child most likely to undergo SSIOAC.^{19,20} Similarly, their eyes are of comparable sizes. Finally, earlier studies identified the macaque as a valid model to study anticancer drug pharmacokinetics.^{22,24,25}

Previous studies have described the complex embryology, anatomic variants, and angiographic techniques to evaluate orbital vasculature.²⁶ In our current study, we sought to validate our NHP model by evaluating the size of the pediatric and adolescent OAs and compare it to the NHP. We found OA measurements of our NHPs to be similar to those in our pediatric population. Quantitative comparison of the OA in pediatric versus adolescent patients demonstrated vascular growth occurring over the first two decades of life. The OA approaches an adult size of approximately 1.4 mm^{27,28} during adolescence, highlighting the pediatric vasculature as a unique and delicate system. Our findings validate our NHP model as a means of studying the toxicities of SSIOAC for the treatment of retinoblastoma.

In our previously published studies, we documented acute ocular vascular toxicities in our NHP model during SSIOAC.^{19,20} Our findings were similar to those reported in children with retinoblastoma treated with SSIOAC. We believe these toxicities result from a complex interaction between drug concentration, drug delivery, inflammatory mediators,

leukostasis, and particulates, with an end result of endothelial cell inflammation and apoptosis. How hemodynamic variables, namely the OA diameter, the diameter of the OA relative to diameter of the microcatheter, and the consequences of intermittent pulsatile perfusion impact these complex interactions requires further investigation. This validation study not only provided additional anatomic detail and precision measurement of the arterial system of the NHP macaque^{23,29,30} but also served as a relevant noncadaveric study^{27,28} of the pediatric OA focusing on a retinoblastoma-pertinent age group—information that is fairly limited in the literature.

Going forth, our data will provide the background for a computational flow model we will use to elucidate the hemodynamic consequences of cannulation and infusion of the OA.

In conclusion, we must appreciate that the drug toxicities and hemodynamic consequences of SSIOAC are not fully known and may be significantly more than previously realized. With this in mind, retinoblastoma specialists are now approaching this treatment with appropriate caution.^{5,13,21} Treatment algorithms for intraocular retinoblastoma will remain in constant flux without more data to support an efficacious delivery and dosing regimen that is safe for the child. Efforts to explore these and other questions are ongoing, and a Children's Oncology Group Trial has been proposed.³¹ In the interim, we will continue our efforts to study and, hopefully, mitigate the observed toxicities.

References

1. Yamane T, Kaneko A, Mohri M. The technique of ophthalmic arterial infusion therapy for patients with intraocular retinoblastoma. *Int J Clin Oncol*. 2004;9:69–73.
2. Abramson DH, Dunkel IJ, Brodie SE, et al. A phase I/II study of direct intraarterial (ophthalmic artery) chemotherapy with melphalan for intraocular retinoblastoma. *Ophthalmology*. 2008;115:1398–1404.
3. Shields CL, Bianciotto CG, Jabbour P, et al. Intra-arterial chemotherapy for retinoblastoma: report No. 1, control of retinal tumors, subretinal seeds, and vitreous seeds. *Arch Ophthalmol*. 2011;129:1399–1406.
4. Gobin YP, Dunkel IJ, Marr BP, Brodie SE, Abramson DH. Intra-arterial chemotherapy for the management of retinoblastoma: four-year experience. *Arch Ophthalmol*. 2011;129:732–737.
5. Shields CL, Bianciotto CG, Jabbour P, et al. Intra-arterial chemotherapy for retinoblastoma: report No. 2, treatment complications. *Arch Ophthalmol*. 2011;129:1407–1415.
6. Munier FL, Beck-Popovic M, Balmer A, et al. Occurrence of sectoral choroidal occlusive vasculopathy and retinal arteriolar embolization after superselective ophthalmic artery chemotherapy for advanced intraocular retinoblastoma. *Retina*. 2011;31:566–573.
7. Peterson EC, Elhammady MS, Quintero Wolfe S, et al. Selective artery infusion of chemotherapy for advanced intraocular retinoblastoma: initial experience with 17 tumors. *J Neurosurg*. 2001;114:1603–1608.
8. Shields CL, Ramasubramanian S, Shah S, et al. Effect of intraarterial chemotherapy on retinoblastoma-induced retinal detachment. *Retina*. 2012;32:799–804.
9. Abramson DH, Marr BP, Brodie SE, Dunkel I, Palioura S, Gobin YP. Ophthalmic artery chemosurgery for less advanced intraocular retinoblastoma: five year review. *PLoS one*. 2012; 7:e34120. doi:10.1371/journal.pone.0034120.
10. Abramson DH, Dunkel IJ, Brodie SE, et al. Superselective ophthalmic artery chemotherapy as primary treatment for retinoblastoma (chemosurgery). *Ophthalmology*. 2010;117: 1623–1629.

11. Abramson DH, Dunkel IJ, Brodie SE, et al. Bilateral superselective ophthalmic artery chemotherapy for bilateral retinoblastoma: tandem therapy. *Arch Ophthalmol*. 2010;128:370-372.
12. Shields CL, Kaliki S, Shah SU, et al. Minimal exposure (one or two cycles) of intra-arterial chemotherapy in the management of retinoblastoma. *Ophthalmology*. 2012;119:188-192.
13. Bianciotto C, Shields CL, Iturralde JC, et al. Fluorescein angiographic findings after intra-arterial chemotherapy for retinoblastoma. *Ophthalmology*. 2012;119:843-849.
14. Marr BP, Gobin PY, Dunkel IJ, et al. Spontaneously resolving periocular erythema and ciliary madarosis following intra-arterial chemotherapy for retinoblastoma. *Middle East Afr J Ophthalmol*. 2010;17:207-209.
15. Shields CL, Ramasubramanian A, Rosenwasser R. Superselective catheterization of the ophthalmic artery for intraarterial chemotherapy for retinoblastoma. *Retina*. 2009;29:1207-1209.
16. Shields CL, Shields JA. Intra-arterial chemotherapy for retinoblastoma: the beginning of a long journey. *Clin Experiment Ophthalmol*. 2010;38:638-643.
17. Shields CL, Shields JA. Retinoblastoma management: advances in enucleation, intravenous chemoreduction, and intra-arterial chemotherapy. *Curr Opin Ophthalmol*. 2010;21:203-212.
18. Vajzovic LM, Murray TG, Aziz-Sultan MA, et al. Supraselective intra-arterial chemotherapy: evaluation of treatment-related complications in advanced retinoblastoma. *Clin Ophthalmol*. 2011;5:171-176.
19. Wilson MW, Jackson JS, Phillips BX, et al. Real-time ophthalmoscopic findings after superselective intraophthalmic artery chemotherapy in a nonhuman primate model. *Arch Ophthalmol*. 2011;129:1458-1465.
20. Steinle JJ, Zhang Q, Thompson KE, et al. Intra-ophthalmic artery chemotherapy triggers vascular toxicity through endothelial cell inflammation and leukostasis. *Invest Ophthalmol Vis Sci*. 2012;53:2439-2445.
21. Wilson MW, Haik BG, Dyer MA. Superselective intraophthalmic artery chemotherapy: what we do not know. *Arch Ophthalmol*. 2011;129:1490-1491.
22. Berg SL, Aleksic A, McGuffey L, et al. Plasma and cerebrospinal fluid pharmacokinetics of rebeccamycin (NSC 655649) in nonhuman primates. *Cancer Chemother Pharmacol*. 2004;54:127-130.
23. Weinstein JD, Hedges TR. Studies of intracranial and orbital vasculature of the rhesus monkey (*Macaca mulatta*). *Anat Rec*. 1962;144:37-41.
24. Berg SL, Stone J, Xiao JJ, et al. Plasma and cerebrospinal fluid pharmacokinetics of depsipeptide (FR901228) in nonhuman primates. *Cancer Chemother Pharmacol*. 2004;54:85-88.
25. Berg S, Serabe B, Aleksic A, et al. Pharmacokinetics and cerebrospinal fluid penetration of phenylacetate and phenylbutyrate in the nonhuman primate. *Cancer Chemother Pharmacol*. 2001;47:385-390.
26. Vignaud J, Hasso AN, Lasjaunias P, Clay C. Orbital vascular anatomy and embryology. *Radiology*. 1974;111:617-626.
27. Perrini P, Cardia A, Fraser K, Lanzino G. A microsurgical study of the anatomy and course of the ophthalmic artery and its possibly dangerous anastomoses. *J Neurosurg*. 2007;106:142-150.
28. Kocabiyyik N, Yazar F, Ozan H. The intraorbital course of ophthalmic artery and its relationship with the optic nerve. *Neuroanatomy*. 2009;8:36-38.
29. Ayajiki K, Tanaka T, Okamura T, Toda N. Evidence for nitroxidergic innervation in monkey ophthalmic arteries in vivo and in vitro. *Am J Physiol Heart Circ Physiol*. 2000;279:H2006-H2012.
30. Netland PA, Siegner SW, Harris A. Color Doppler ultrasound measurements after topical and retrobulbar epinephrine in primate eyes. *Invest Ophthalmol Vis Sci*. 1997;38:2655-2661.
31. Levin MH, Gombos DS, O'Brien JM. Intra-arterial chemotherapy for advanced retinoblastoma: is the time right for a prospective clinical trial? *Arch Ophthalmol*. 2011;129:1487-1489.